AEM
Journals.ASM.org

Effects of Metal Ions on Stability and Activity of Hyperthermophilic Pyrolysin and Further Stabilization of This Enzyme by Modification of a Ca^{2+}-Binding Site

Jing Zeng,[a] Xiaowei Gao,[a] Zheng Dai,[a] Bing Tang,[a,b] Xiao-Feng Tang[a,b]

State Key Laboratory of Virology, College of Life Sciences, Wuhan University, Wuhan, China[a]; Hubei Provincial Cooperative Innovation Center of Industrial Fermentation, Wuhan, China[b]

Pyrolysin is an extracellular subtilase produced by the marine hyperthermophilic archaeon *Pyrococcus furiosus*. This enzyme functions at high temperatures in seawater, but little is known about the effects of metal ions on the properties of pyrolysin. Here, we report that the supplementation of Na^+, Ca^{2+}, or Mg^{2+} salts at concentrations similar to those in seawater destabilizes recombinant pyrolysin but leads to an increase in enzyme activity. The destabilizing effect of metal ions on pyrolysin appears to be related to the disturbance of surface electrostatic interactions of the enzyme. In addition, mutational analysis of two predicted high-affinity Ca^{2+}-binding sites (Ca1 and Ca2) revealed that the binding of Ca^{2+} is important for the stabilization of this enzyme. Interestingly, Asn substitutions at residues Asp818 and Asp820 of the Ca2 site, which is located in the C-terminal extension of pyrolysin, resulted in improvements in both enzyme thermostability and activity without affecting Ca^{2+}-binding affinity. These effects were most likely due to the elimination of unfavorable electrostatic repulsion at the Ca2 site. Together, these results suggest that metal ions play important roles in modulating the stability and activity of pyrolysin.

Hyperthermophiles grow optimally at temperatures of 80°C or higher (1), and some can survive and reproduce at temperatures higher than 120°C (2, 3). Enzymes from hyperthermophiles are especially valuable for probing the stabilization mechanisms that allow proteins to function near the maximum temperature of life, and studying these enzymes also offers insight into opportunities to greatly expand the reaction conditions of biocatalysis (4–6). At high temperatures, inactivation of enzymes occurs mainly due to thermal denaturation (loss of tertiary structure) and degradation (loss of primary structure) (7). Accumulating evidence suggests that hyperthermophilic enzymes have evolved multiple mechanisms to adapt to hyperthermal environments; however, no general rules for stabilization of these enzymes have been described (5, 8). Known intrinsic stabilization factors include improved hydrophobic and aromatic interactions, increased ionic interactions, decreased entropy of the unfolded state and solvent-accessible hydrophobic surface, anchoring of loose ends, intersubunit interactions and oligomerization, metal binding, and posttranslational modifications (5, 8–11). Certain hyperthermophiles possess a specific protein disulfide oxidoreductase and use disulfide bonding as a major mechanism for protein stabilization (12, 13). In addition to the intrinsic factors, some hyperthermophilic enzymes are stabilized by extrinsic factors, such as intracellular compatible solutes and molecular chaperones, ligand binding, crowding effects inside the cells, and association with the surface layer (S-layer) (5, 8, 14, 15). Although hyperthermophilic enzymes have become model systems to investigate mechanisms of enzyme stabilization and have provided the rational basis for improving the stability of less stable enzymes, few attempts have been made to further stabilize hyperthermophilic enzymes. Genetic engineering of hyperthermophilic enzymes and selection of mutants with higher stability will ultimately aid our understanding of the upper temperature limits for enzyme activity and stability (5).

The marine hyperthermophilic archaeon *Pyrococcus furiosus*, which grows optimally at 100°C (16), is highly proteolytic and requires peptides for growth (17–20). Pyrolysin is an extracellular serine protease that was isolated from the cell envelope fraction of *P. furiosus* and characterized as an extremely stable enzyme with optimal caseinolytic activity at 115°C and a half-life of 4 h at 100°C (19). This enzyme is synthesized as a precursor (1,398 residues) containing a signal peptide (26 residues), an N-terminal propeptide (123 residues), a subtilisin-like catalytic domain with a large insert of 147 residues (Is147), and a long C-terminal extension (CTE; ~740 residues) (6, 21). The molecular architecture of pyrolysin is a mosaic of domains that is shared by other hyperthermophilic proteases, such as stetterlysin from *Thermococcus stetteri* (6) and the stalk-associated archaebacterial endoprotease (STABLE protease) from *Staphylothermus marinus* (15). These enzymes are grouped together into the pyrolysin family of subtilases (22). As one of the most thermostable proteases, pyrolysin is an ideal model for investigating the mechanisms of enzyme stability and activity near the maximum temperature of life. A previous study showed that pyrolysin activity was partially inhibited by EDTA and that this inhibition could be overcome by the addition of $CaCl_2$ (19). Based on the evidence that native pyrolysin is glycosylated, Voorhorst et al. (21) proposed that posttranslational modification may function in the thermostabilization of this enzyme. In addition, the comparison of the predicted three-dimen-

Received 2 January 2014 **Accepted** 16 February 2014
Published ahead of print 21 February 2014
Editor: R. M. Kelly
Address correspondence to Xiao-Feng Tang, tangxf@whu.edu.cn.
Supplemental material for this article may be found at http://dx.doi.org/10.1128/AEM.00006-14.

doi:10.1128/AEM.00006-14

sional model of the catalytic domain of pyrolysin with structures of subtilases of psychrophilic, mesophilic, and thermophilic origin revealed possible intrinsic factors for pyrolysin stabilization, including increased surface ionic and aromatic interactions, and the presence of some Ca^{2+}-binding ligands (6); however, these possible intrinsic factors have yet to be confirmed experimentally.

Recently, we successfully expressed the pyrolysin proform (Pls) in *Escherichia coli* (23), and enzyme maturation was found to occur via autoprocessing of both the N- and C-terminal propeptides at high temperatures to generate the mature pyrolysin (mPls), which consists of the catalytic domain and a C-terminal extension (CTEm; ~ 540 residues). Deletion mutation analysis of Pls suggests that both of the propeptides assist in achieving pyrolysin hyperthermostability and that CTEm not only confers additional stability to mPls but also improves its catalytic efficiency for both proteinaceous and small synthetic peptide substrates (23). In agreement with the previous study on native pyrolysin (19), the stability of recombinant pyrolysin was decreased in the presence of EDTA, reemphasizing the importance of metal binding in enzyme stability. Our attempts to purify the recombinant pyrolysin by ion-exchange chromatography, however, were unsuccessful due to the fact that this protein tended to precipitate as the NaCl concentration increased. These observations prompted us to explore the underlying mechanism for the salt response of pyrolysin. In this study, the effects of different salts on the maturation and enzyme properties of pyrolysin were investigated, revealing that metal ions play an important role in modulating both the stability and the activity of this enzyme. Several residues that were predicted to be involved in Ca^{2+} binding in pyrolysin were subjected to mutational analysis, and these experiments demonstrated that two predicted Ca^{2+}-binding sites (Ca1 and Ca2) contribute to the thermostability of pyrolysin. Interestingly, the removal of charged carboxyl groups in the Ca2 site within the CTE of pyrolysin increased both the stability and the activity of the enzyme.

MATERIALS AND METHODS

Strains and growth conditions. *E. coli* DH5α and *E. coli* BL21-CodonPlus(DE3)-RIL were used as hosts for cloning and protein expression. Bacteria were grown at 37°C in Luria-Bertani (LB) medium containing chloramphenicol (34 μg/ml) and/or kanamycin (30 μg/ml), as needed.

Plasmid construction and mutagenesis. The expression plasmids for the proforms of wild-type (WT) pyrolysin Pls (pET26b-*pls*) and its active-site mutant PlsS441A (pET26b-*plsS441A*) were constructed previously (23). The genes encoding the CTE-deletion mutant PlsΔC740b and the CTE fragment PlsC740b were amplified by PCR from the pET26b-*pls* template with the primer pairs listed in Table S1 in the supplemental material, and the products were then inserted into pET26b to generate the expression plasmids pET26b-*plsΔC740b* and pET26b-*plsC740b* (see Table S2 in the supplemental material). The recombinants PlsΔC740b and PlsC740b were used for preparation of antibodies in this study (see below) and differ from previously described PlsΔC740 and PlsC740 (23) in that the last two contain a His tag at the C terminus.

The QuikChange site-directed mutagenesis (SDM) method (24) was employed to construct the pyrolysin Ca^{2+}-binding-site mutants using the primers listed in Table S1 in the supplemental material. The plasmid pET26b-*pls* was subjected to single SDM or successive rounds of SDM to generate a series of single, double, and triple mutants (see Table S2 in the supplemental material). All the recombinant plasmids were confirmed by DNA sequencing.

Expression, activation, and purification. Expression of the recombinant proteins in *E. coli* BL21-CodonPlus(DE3)-RIL was carried out as described previously (23). Then, the harvested cells were suspended in buffer A (20 mM HEPES, 10 mM NaOH, pH 7.5) containing 0.5 M NaCl and disrupted by sonication, followed by centrifugation at 13,000 × *g* for 10 min. The insoluble fractions were recovered and dissolved in buffer A containing 6 M urea, incubated at 4°C overnight, and then subjected to centrifugation at 13,000 × *g* for 10 min. The resulting supernatants were dialyzed against buffer A overnight at 4°C to remove the urea and were then used as crude protein samples. For purification of PlsS441A, the insoluble fraction containing PlsS441A fused with a His tag was dissolved in buffer A containing 6 M urea and then subjected to affinity chromatography on an Ni^{2+}-charged chelating Sepharose Fast Flow resin (GE Healthcare) column equilibrated with buffer A containing 6 M urea. After washing the column with buffer A containing 40 mM imidazole and 6 M urea, the bound PlsS441A was eluted with buffer A containing 300 mM imidazole and 6 M urea. The eluted sample was dialyzed against buffer A to remove the imidazole and urea and then stored at 4°C until use.

To prepare the mature enzymes, crude samples of the proforms (Pls and its mutants) in buffer A were incubated at 95°C for 2 h to activate the enzymes. The resulting mature enzymes were subjected to affinity chromatography on a bacitracin-Sepharose 4B (Amersham Biosciences, Sweden) column equilibrated with buffer A. After washing with buffer A containing 6 M urea, the bound enzymes were eluted with buffer A containing 6 M urea and 20% isopropanol. Notably, pyrolysin is resistant to high concentrations of urea, and 6 M urea was included in the washing and elution buffers in order to reduce nonspecific protein binding to the affinity resins. Finally, the eluted fractions containing the purified enzymes were dialyzed against buffer A to remove urea and isopropanol. The enzyme solution was concentrated with a Micron YM-3 centrifugal filter (Amicon, Beverly, MA) as needed. The concentrations of the purified protein samples were determined using the Bradford method (25) with bovine serum albumin (BSA) as the standard.

SDS-PAGE, gelatin overlay assay, and immunoblot analysis. SDS-PAGE was performed with the Tris-glycine buffer system (26). The samples for conventional SDS-PAGE analysis were precipitated with 20% (wt/vol) trichloroacetic acid (TCA), washed with acetone, solubilized in a loading buffer containing 8 M urea, and then subjected to electrophoresis without prior heat treatment. For activity staining of the protease, the samples were mixed with the loading buffer without urea and then examined in a gelatin overlay assay, which was performed according to the method described by Blumentals et al. (17), except that the proteolytic reaction was carried out at 90°C for 2 h in buffer A. The recombinants PlsΔC740b and PlsC740b were used as antigens for the generation of antibodies in rabbits. Antiserum against PlsΔC740b (anti-NM) or PlsC740b (anti-C) was prepared and used for immunoblot analysis according to the method described previously (27).

Enzymatic activity assay. Unless otherwise indicated, the azocaseinolytic activity of the enzyme was assayed at 95°C for 30 min in a 400-μl reaction mixture that contained 0.25% (wt/vol) azocasein (Sigma) and 200 μl of enzyme sample in buffer A. The reaction was terminated by the addition of 400 μl of 40% (wt/vol) TCA. After incubation at room temperature for 15 min, the mixture was centrifuged at 13,000 × *g* for 10 min, and the absorbance of the supernatant was measured at 335 nm in a 1-cm-light-path cell. One unit (U) of activity was defined as the amount of enzyme required to increase the A_{335} value by 0.01 per min. To determine the activity of the enzyme in artificial seawater (ASW), 20 μl of enzyme sample in buffer A was diluted with 180 μl of ASW (450 mM NaCl, 10 mM KCl, 9 mM $CaCl_2$, 30 mM $MgCl_2$, 16 mM $MgSO_4$, pH 7.8) (28) and then mixed with 200 μl of 0.5% (wt/vol) azocasein in ASW. The samples were then assayed for enzymatic activity as described above. For activity assays at temperatures above 100°C, the reaction was carried out in screw-top tubes with O rings to prevent evaporation, and a glycerol bath was used.

The enzymatic activity of the protease on the substrate *N*-succinyl–Ala–Ala–Pro–Lys–*p*-nitroanilide (suc-AAPK-pNA; GL Biochem Ltd., Shanghai, China) was measured at the temperatures indicated below in buffer A containing 0.5 mM substrate. The activity was recorded by monitoring the initial velocity of suc-AAPK-pNA hydrolysis at 410 nm in a

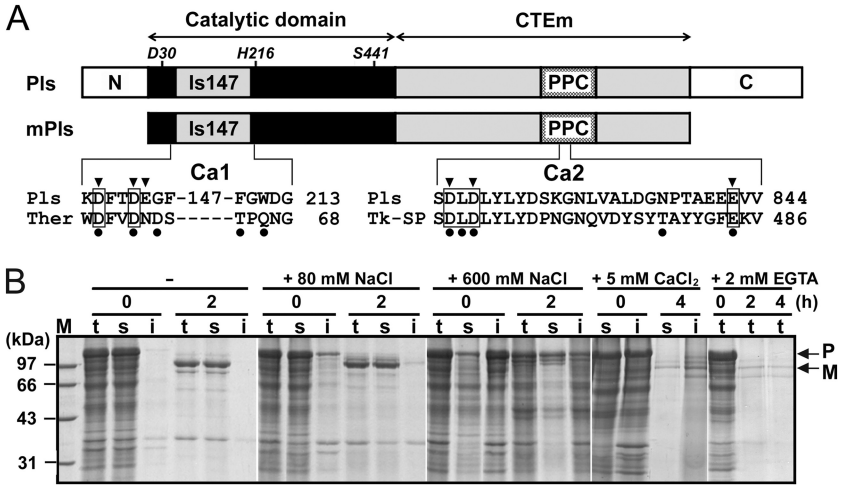

FIG 1 Schematic representation of the primary structure of pyrolysin and SDS-PAGE analysis of the effects of metal ions on its maturation. (A) The regions of the catalytic domain and CTEm are indicated by double-headed arrows. The locations of the active-site residues (Asp30, His216, and Ser441) are shown. N and C represent the N- and C-terminal propeptides, respectively. The positions of the large insert (Is147) and the PPC domain are indicated. The alignments of amino acid sequences around the two predicted Ca^{2+}-binding sites (Ca1 and Ca2) of pyrolysin with those of thermitase (Ther) and Tk-SP subtilisin (Tk-SP) are shown at the bottom. The residues of the Ca2 site of thermitase (PDB accession number 2TEC) and the Ca1 site of Tk-SP subtilisin (PDB accession number 3AFG) are indicated by filled circles. Conserved Ca^{2+}-binding residues are boxed. The residues of pyrolysin that were subjected to mutagenesis analysis are indicated by arrowheads. (B) Crude samples of Pls in buffer A without (−) or with (+) 80 or 600 mM NaCl, 5 mM $CaCl_2$, or 2 mM EGTA were incubated at 95°C. At the time intervals indicated, samples (lanes t) were withdrawn and the soluble (lanes s) and insoluble (lanes i) fractions were separated by centrifugation and subjected to SDS-PAGE analysis. The positions of Pls (P) and mPls (M) on the gels are indicated by arrows. Lane M, molecular mass markers.

thermostated spectrophotometer (Cintra 10e; GBC, Australia). This velocity was calculated on the basis of an extinction coefficient for *p*-nitroaniline (pNA) of 8,480 M^{-1} cm^{-1} at 410 nm (29).

N-terminal sequencing. After separation by SDS-PAGE, the proteins were electroblotted onto a polyvinylidene difluoride membrane and then stained with Coomassie brilliant blue R-250. The target protein bands were excised and subjected to N-terminal amino acid sequence analysis using a PPSQ-33A protein sequencer (Shimadzu).

RESULTS

Effects of metal ions on maturation of pyrolysin. At high temperatures, Pls is converted to mPls via autoprocessing of both the N- and C-terminal propeptides (Fig. 1A). In previous studies, a phosphate buffer system was used to characterize this enzyme (19, 21, 23); however, this buffer system is not suitable for investigation of the effects of metal ions on pyrolysin properties because the addition of multivalent metal ions to phosphate buffer forms insoluble phosphate precipitates. Thus, we employed a HEPES buffer system (20 mM HEPES, 10 mM NaOH, pH 7.5 [buffer A]) to investigate the effects of metal ions on pyrolysin maturation. As shown in Fig. 1B, Pls was converted into mPls following incubation at 95°C for 2 h in buffer A. The yield of mPls, however, decreased with the increase in NaCl concentration. Similarly, the addition of 5 mM $CaCl_2$ into buffer A also led to a low yield of mPls. These results indicate that the addition of salts in buffer A is unfavorable for the maturation of Pls.

We noticed that Pls remained in a soluble form in the absence of supplemental salts but tended to precipitate as the NaCl concentration was increased or in the presence of $CaCl_2$ (Fig. 1B). To investigate whether the precipitation of Pls is caused by salt-induced destabilization of the proform, purified active-site mutant proform PlsS441A was incubated at room temperature or at 95°C with different concentrations of salts. After incubation for 2 h, almost all of the PlsS441A precipitated in the presence of 600 mM NaCl, 10 mM $CaCl_2$, or 50 mM $MgCl_2$ or in ASW (Fig. 2A). The fact that precipitation occurred at low concentrations of $CaCl_2$ or $MgCl_2$ but only at relatively high concentrations of NaCl implied that the proform is more sensitive to $CaCl_2$ and $MgCl_2$ than to NaCl. Interestingly, the precipitates that formed at room temperature could be partially resolubilized in buffer A at room temperature, while those formed at 95°C could not be resolubilized (Fig. 2B). In addition, the precipitates formed at room temperature were also unable to be resolubilized in buffer A at 95°C (data not shown). The irreversible aggregation of the proform at high tem-

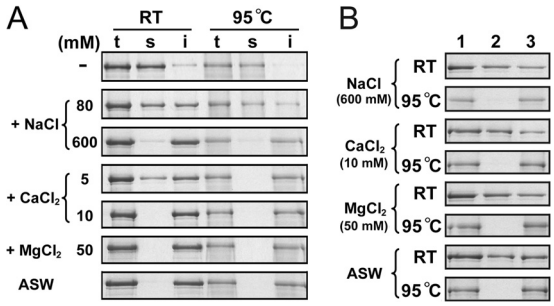

FIG 2 SDS-PAGE analysis of the effects of metal ions on the solubility of PlsS441A. (A) Salt-induced precipitation formation of PlsS441A. Purified PlsS441A (50 nM) in buffer A with (+) or without (−) various concentrations of NaCl, $CaCl_2$, or $MgCl_2$ or in ASW were incubated at room temperature (RT) or 95°C. After 2 h, samples (lanes t) were withdrawn, and the soluble (lanes s) and insoluble (lanes i) fractions were separated by centrifugation and subjected to SDS-PAGE analysis. (B) Resolubilization of PlsS441A precipitate. The insoluble fractions (lane 1) of PlsS441A that formed in buffer A (200 μl) with the indicated concentration (in parentheses) of different salts, as well as that formed in ASW at room temperature or 95°C, were resuspended in 200 μl of buffer A. After incubation at room temperature for 2 h, the soluble (lane 2) and insoluble (lane 3) fractions were separated as described for panel A and subjected to SDS-PAGE analysis.

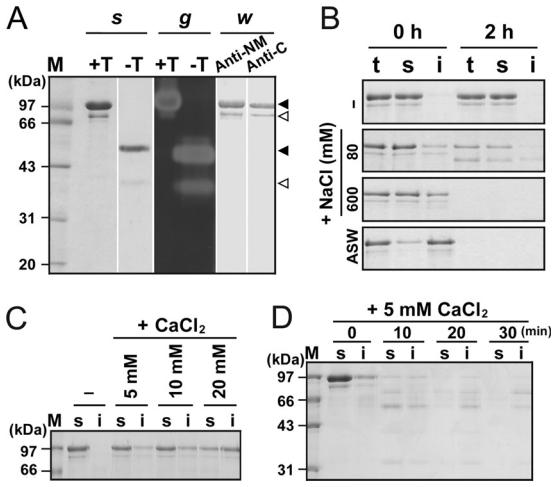

FIG 3 Effects of metal ions on enzymatic properties of mPls. (A) SDS-PAGE, gelatin overlay assay, and immunoblot analysis of the purified mPls. The enzyme sample before (lanes −T) or after (lanes +T) TCA precipitation was subjected to SDS-PAGE analysis (*s*), followed by gelatin overlay assay at 90°C (*g*). The TCA-precipitated mPls was also subjected to Western blot analysis (*w*) using antibodies against the N-terminal propeptide and the catalytic domain (lane anti-NM) and antibodies against the CTE of Pls (lane anti-C). The major and minor species in the purified sample are indicated by black and white arrowheads, respectively. (B to D) Salt-induced precipitation formation and degradation of mPls. The enzyme samples (50 nM) in buffer A with (+) or without (−) various concentrations of NaCl or $CaCl_2$ or in ASW were incubated at room temperature for 2 h (C) or at 95°C for the time intervals indicated (B and D). Then, samples (lanes t) were withdrawn, and the soluble (lanes s) and insoluble (lanes i) fractions were separated by centrifugation and then subjected to SDS-PAGE analysis. Lanes M, molecular mass markers.

peratures suggests that the precipitation of the proform is mainly due to its destabilization by the supplemental salts, resulting in a low maturation efficiency of the enzyme. However, Pls does require metal ions for proper maturation, as evidenced by the fact that the presence of 2 mM EGTA significantly decreased the yield of mPls at 95°C (Fig. 1B). One reasonable explanation for this finding is that pyrolysin possesses a high-affinity metal ion-binding site(s), which is occupied even at extremely low salt concentrations and contributes to the structural stability of Pls, and thus, the removal of metal ions from the binding site(s) by chelating agents destabilizes the proform.

Effects of metal ions on stability and activity of mPls. To prepare the mature form for analysis of enzyme properties, Pls was subjected to heat treatment (95°C) in buffer A, and the mature form was purified by affinity chromatography. As shown in Fig. 3A, the TCA-treated purified sample contained not only the 100-kDa mPls but also a minor species (named Md) with an apparent molecular size of ~80 kDa, and the two species without TCA treatment exhibited apparent molecular sizes of 55 and 40 kDa, respectively. In a gelatin overlay assay, the two species without TCA treatment exhibited proteolytic activity, but the TCA-treated Md showed much weaker activity than the TCA-treated mPls (Fig. 3A), implying that Md is less resistant to TCA treatment than mPls. In addition, the two species were detected with anti-NM and anti-C antibodies (Fig. 3A), indicating that both of these molecules contain the catalytic domain and at least part of the C-terminal extension. The first four residues of the two species were identified as MYNS by N-terminal sequencing, suggesting that Md represents an mPls degradation product via C-terminal truncation.

To investigate the effects of metal ions on enzyme stability, mPls was incubated with different concentrations of NaCl or $CaCl_2$. Similar to the proform, mPls remained in a soluble form after incubation at 95°C for 2 h in the absence of supplemental salts but tended to precipitate with the increase of the NaCl concentration and experienced autodegradation (Fig. 3B). The mature form also tended to precipitate at room temperature as the $CaCl_2$ concentration increased (Fig. 3C) and was autodegraded during incubation with 5 mM $CaCl_2$ at 95°C (Fig. 3D). However, we noticed that the majority of mPls remained in a soluble form when incubated with 5 to 10 mM $CaCl_2$ at room temperature for 2 h (Fig. 3C), while most or all of the proform molecules precipitated under the same conditions (Fig. 2A). Similarly, the level of the soluble form of mPls was higher than that of the proform when incubated with 80 to 600 mM NaCl at room temperature for 2 h (data not shown). Our previous study demonstrated that the proform is less stable than mPls (23). The difference in their sensitivities to salt-induced precipitation likely reflects this difference in stability between mPls and the proform. Notably, in the presence of salts or in ASW, both the soluble and insoluble forms of mPls experienced autodegradation at 95°C (Fig. 3B and D). These results suggest that the presence of salts not only induces the precipitation of the mature form but also affects its thermostability.

The effect of metal ions on the enzymatic activity of the mature

TABLE 1 Effects of metal ions on activity of pyrolysin

Salt	Concn (mM)	Relative activity[a] (%)
None		100
NaCl	80	167.8 ± 1.5
	600	280.1 ± 4.7
$NaNO_3$	80	172.8 ± 1.2
	600	299.2 ± 0.6
Na_2SO_4	40	173.1 ± 3.3
	300	278.3 ± 1.6
$CaCl_2$	0.01	102.3 ± 2.2
	0.1	106.5 ± 1.6
	1	142.8 ± 2.3
	5	227.5 ± 1.8
	10	248.5 ± 0.4
$Ca(NO_3)_2$	1	150.6 ± 0.4
	5	233.8 ± 3.6
	10	247.1 ± 3.3
$MgCl_2$	5	179.2 ± 2.0
	50	232.0 ± 1.3
$Mg(NO_3)_2$	5	197.6 ± 1.8
	50	230.0 ± 1.1
$MgSO_4$	5	201.7 ± 1.5
	50	244.4 ± 1.4
ASW		180.0 ± 4.2

[a] Enzyme activity was measured at 95°C using 0.5% azocasein as the substrate in buffer A with different concentrations of salts or in ASW. The relative activity was calculated on the basis of the measured activity in the absence of supplemental salts (defined as 100%). The values are expressed as means ± standard deviations of triplicate measurements.

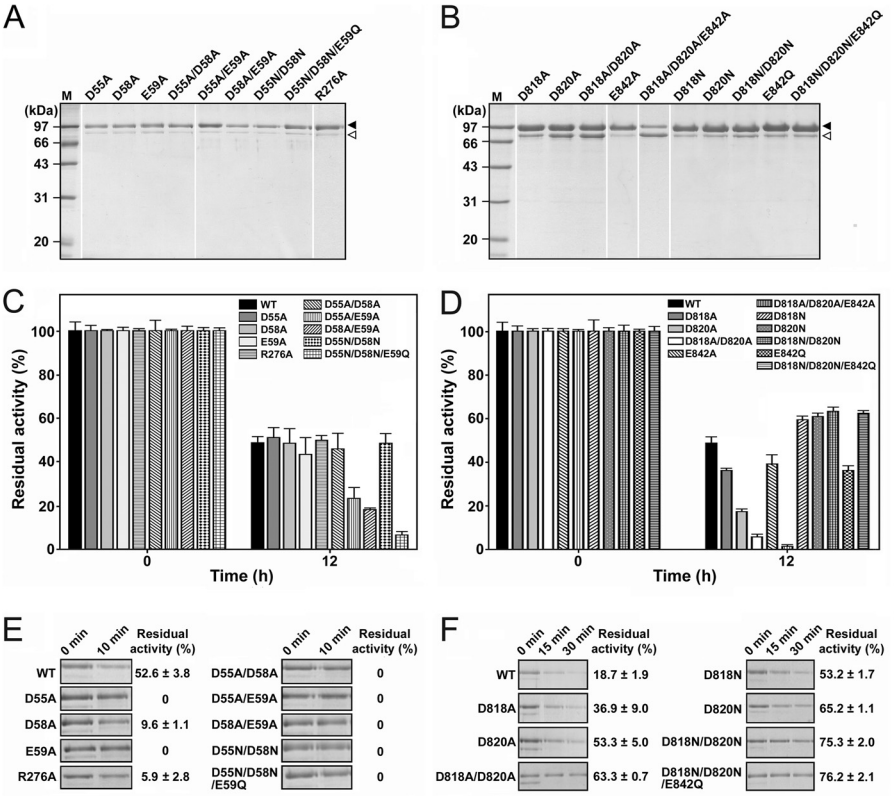

FIG 4 Effects of mutation of the residues of Ca1 (A, C, and E) and Ca2 (B, D, and F) on pyrolysin stability. (A and B) SDS-PAGE analysis of the purified samples of the mature mutants. The major and minor species in the purified enzyme sample are indicated by black and white arrowheads, respectively. Lanes M, molecular mass markers. (C to F) Thermal stability of the mutants. The purified samples of mPls and its mutants (5.0 μg/ml) in buffer A were incubated at 95°C in the absence (C and D) or presence (E and F) of 2 mM EDTA. At the time intervals indicated, samples were withdrawn and subjected to an azocaseinolytic activity assay (C to F) and SDS-PAGE analysis (E and F). The residual activity is expressed as a percentage of the original activity of each enzyme sample. The values are expressed as means ± SDs (bars) of the results of three independent experiments.

form was then investigated. As shown in Table 1, the mature form displayed enhanced activity in the presence of different Na^+, Ca^{2+}, and Mg^{2+} salts, and the activity level increased with the increase of the salt concentrations. Meanwhile, the enhancement of enzyme activity was observed at lower levels of Ca^{2+} and Mg^{2+} salts (<~50 mM) and at relatively high levels of Na^+ salts (~600 mM). In ASW, the activity of the mature form was also increased by ~80%. Moreover, the mature form exhibited similar activity levels at the same concentrations of NaCl and $NaNO_3$, and a similar result was also observed for Ca^{2+} and Mg^{2+} salts (Table 1), indicating that the enzyme activity depends on the metal ions rather than the anions. Taken together, these results suggest that although supplemental metal ions (e.g., Na^+, Ca^{2+}, and Mg^{2+}) lead to the destabilization of the mature form, the presence of these metal ions actually promotes the activity of this enzyme.

Mutational analysis of the Ca1 site of pyrolysin. The results presented above showed that Ca^{2+} plays important roles in the maturation, stability, and activity of pyrolysin. As shown in Fig. 1A, pyrolysin possesses at least two possible Ca^{2+}-binding sites (Ca1 and Ca2). The Ca1 site of pyrolysin was previously predicted to correspond to the Ca2 site of thermitase (6, 30, 31). Two of the five ligand residues at the Ca2 site of thermitase are conserved in pyrolysin (Asp55 and Asp58; Fig. 1A). In addition, the Arg276 residue of pyrolysin was predicted to contribute to the formation of the Ca1 site through ionic interactions with Asp55 and Asp58 (6). We further postulated that the negatively charged residue Glu59, which is not conserved in thermitase but is near Asp55 and Asp58 in pyrolysin, also contributes to Ca^{2+} binding. Therefore, the Asp55, Asp58, Glu59, and Arg276 residues were selected for mutation to generate single, double, and triple mutants to identify those that are important for Ca^{2+} binding and the thermal stability of pyrolysin.

The purified mature forms of the Ca1 mutants (Fig. 4A) were heat treated at 95°C for 12 h, and the residual activities were measured (Fig. 4C). The single mutants (the D55A, D58A, and R276A mutants) displayed levels of residual activity similar to the level of the WT mPls, while the E59A mutant exhibited a slightly lower level of residual activity (Fig. 4C). When incubated with 2 mM EDTA at 95°C for 10 min, the D55A and E59A mutants were completely inactivated, while the other two single mutants, the D58A and R276A mutants, retained only 9.6% and 5.9% of their original activities, respectively. In contrast, the WT displayed a residual activity of 52.6% (Fig. 4E). This result indicates that all of the four mutated residues are important for the Ca^{2+} binding required to stabilize the enzyme.

All of the mutants with a mutation at Glu59 (the E59A, D55A/E59A, D58A/E59A, and D55N/D58N/E59Q mutants) were less stable than the WT under nonchelating conditions (Fig. 4C). The D55A/D58A/E59A triple mutant was also constructed, but its proform was unable to mature at 95°C (data not shown), although the D55A/D58A double mutant not only was capable of maturation at

95°C but also exhibited thermal stability similar to that of the WT in the absence of chelating agents. The Glu59 residue appeared to play a critical role in maintaining the thermal stability of pyrolysin under nonchelating conditions. After incubation with 2 mM EDTA at 95°C for 10 min, the amount of the Ca1 mutants remained almost unchanged or was decreased to a lesser extent (the D58A and R276A mutants) than that of the WT, although these Ca1 mutants were almost completely inactivated (Fig. 4E). One reasonable explanation for this observation is that the WT was more resistant to EDTA treatment than the mutants but suffered autodegradation during the incubation at 95°C, while the mutants did not show significant autodegradation because Ca^{2+} was more easily chelated from them by EDTA, leading to their rapid destabilization and inactivation. Taken together, Asp55, Asp58, Glu59, and Arg276 are involved in Ca^{2+} binding at the Ca1 site, which plays an important role in maintaining the structural stability of pyrolysin at high temperatures.

Mutational analysis of the Ca2 site of pyrolysin. The pyrolysin Ca2 site, which corresponds to the Ca1 site of the Tk-SP subtilisin from *Thermococcus kodakarensis* KOD1 (32), is located in a putative prepeptidase C-terminal domain (PPC), which exhibits ~25% sequence identity with the β-jelly roll domain of Tk-SP subtilisin (23). Four of the five ligand residues at the Ca1 site of Tk-SP subtilisin are conserved in pyrolysin (Asp818, Leu819, Asp820, and Glu842; Fig. 1A). The three negatively charged residues Asp818, Asp820, and Glu842 were selected for construction of single, double, and triple mutants. The proforms of the mutants were heat treated at 95°C to activate the enzymes, and the mature forms were purified for investigation of the role of the Ca2 site in stabilization of pyrolysin.

Thus, alanine-scanning mutagenesis was employed to investigate the importance of the Ca2 site residues for the thermal stability of pyrolysin. The results of SDS-PAGE analysis revealed that the purified Ala substitution mutants (the D818A, D820A, D818A/D820A, and D818A/D820A/E842A mutants) contained not only the 100-kDa mature form but also increased levels of the 80-kDa Md (Fig. 4B). In the case of the D818A/D820A/E842A mutant, the amount of the 80-kDa Md exceeded that of the 100-kDa mature form, implying that mutation of these residues in pyrolysin affected the structural stability of the enzyme and rendered the enzyme more easily truncated to the 80-kDa Md form. Compared with the WT, all of the Ala substitution mutants showed a significant decrease in residual activity following heat treatment at 95°C for 12 h (Fig. 4D). The fact that the single mutants (the D818A, E842A, and D820A mutants) were more heat resistant than the D818A/D820A double mutant, which was more resistant than the D818A/D820A/E842A triple mutant, suggests that each individual mutation cumulatively destabilizes pyrolysin. These results indicate that residues Asp818, Asp820, and Glu842 also play important roles in stabilizing pyrolysin.

To further explore the roles of the negative charges of the Asp818, Asp820, and Glu842 residues in pyrolysin stability, Asp was changed to Asn, while Glu was mutated to Gln in this enzyme. Unexpectedly, while the E842Q mutant showed a decreased level of residual activity (~35%) compared to the WT (~50%) after heat treatment at 95°C for 12 h, the D818N, D820N, D818N/D820N, and D818N/D820N/E842Q mutants displayed a higher level of residual activity (~60%) under the same conditions (Fig. 4D). When incubated with 2 mM EDTA at 95°C for 30 min, the Asn substitution mutants (the D818N, D820N, D818N/D820N, and D818N/D820N/E842Q mutants) as well as the Ala substitution mutants (the D818A, D820A, and D818A/D820A mutants) exhibited a higher level of residual activity (~37 to 76%) than the WT (~19%) and experienced autodegradation to a lesser extent than the WT (Fig. 4F). These results suggest that the absence of the charged carboxyl groups at the Ca2 site, particularly at Asp818 and Asp820, leads to an increase in the thermostability of pyrolysin.

Enzymatic properties of the D818N/D820N mutant. To investigate the effect of the Asn substitutions at residues Asp818 and Asp820 on the enzymatic properties of pyrolysin, we compared the mature forms of the D818N/D820N mutant and the WT in terms of stability and activity. When incubated at 95°C, the D818N/D820N mutant and WT exhibited half-lives of 18 h and 12 h, respectively (Fig. 5A). Furthermore, heat inactivation of the enzymes at 100 to 115°C resulted in retention of a higher level of original activity by the D818N/D820N mutant than the WT (Fig. 5B). The D818N/D820N mutant displayed higher specific activity toward azocasein than the WT over the temperature range of 50 to 110°C (Fig. 5C). Meanwhile, the D818N/D820N mutant also showed a higher initial velocity of hydrolysis of suc-AAPK-pNA than the WT with this increase in temperature (Fig. 5D). In addition, the azocaseinolytic activity of the D818N/D820N mutant was increased by ~140% in ASW (data not shown), and this activity was higher than that of the WT under the same conditions (an ~80% increase; Table 1). These results suggest that the Asn substitutions at Asp818 and Asp820 lead to not only an increase in the thermostability of pyrolysin but also enhancement of its activity.

We then investigated whether the increase in thermostability of the D818N/D820N mutant was due to increased Ca^{2+} affinity. Because pyrolysin tends to precipitate in the presence of supplemental Ca^{2+}, the determination of the Ca^{2+}-binding constants by the Ca^{2+} titration method was not feasible. Alternatively, the half-lives of the D818N/D820N mutant and WT were determined as a function of the chelator (EDTA or EGTA) concentration at 95°C to assess the contribution of the mutations to Ca^{2+} binding and the increased thermostability of the enzyme. Increasing the concentration of the chelating agent decreased the half-lives of both enzymes, and the dependence of the half-life on the negative log of the EGTA or EDTA concentration was sigmoidal. For the D818N/D820N mutant, the midpoints occurred at 7.2 and 5.4 μM EGTA and EDTA, respectively, and these values were similar to those obtained for the WT, which exhibited midpoints at 7.0 and 5.0 μM EGTA and EDTA, respectively. Given that the shift in the curve reflects a difference in the apparent affinity of the enzyme for Ca^{2+}, the Asn substitutions at Asp818 and Asp820 of pyrolysin are unlikely to cause a significant change in its Ca^{2+} affinity. Nevertheless, the D818N/D820N mutant displayed a longer half-life than the WT at each chelator concentration (Fig. 6).

DISCUSSION

Metal ions induce destabilization of pyrolysin. The destabilizing effect of salts on pyrolysin appears to be related to a disturbance of the surface charge-charge interactions of the enzyme. Compared with its mesophilic and thermophilic homologs, the catalytic domain core of pyrolysin contains an increased number of charged residues that are involved in pairs and networks of charge-charge interactions on the enzyme surface (6). Here, we demonstrate that the disruption of one of the surface ion pair networks (formed among the residues Asp55, Asp58, and Arg276) of pyrolysin by

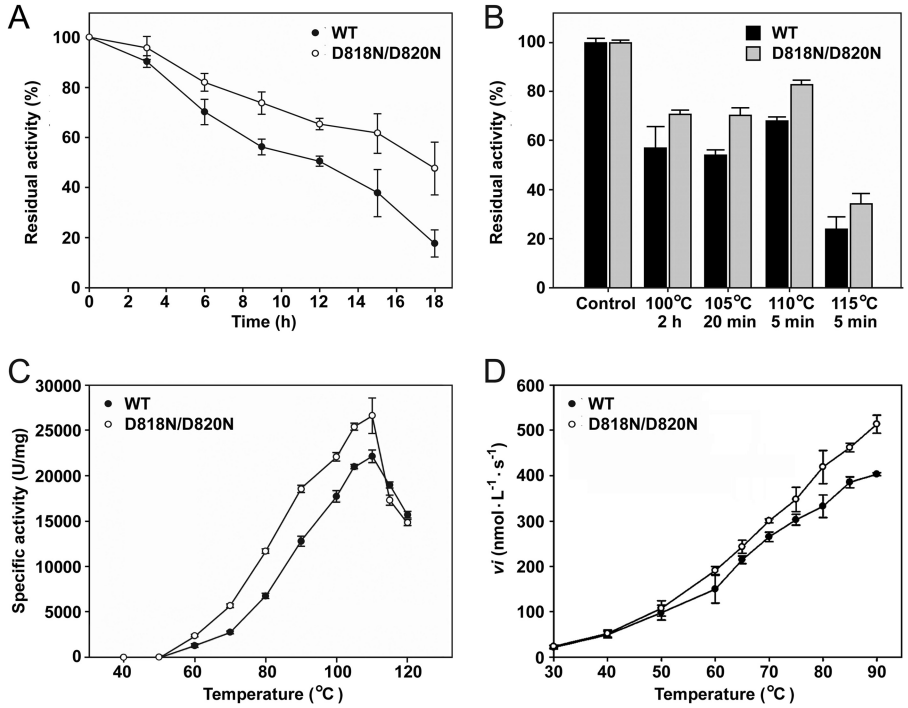

FIG 5 Properties of the WT and the D818N/D820N mutant. (A and B) Heat inactivation of the enzymes. The purified samples of the enzymes (5.0 μg/ml) in buffer A were incubated at 95°C (A) or at 100 to 115°C (B) for the time intervals indicated and then subjected to an azocaseinolytic activity assay. The residual activity was calculated on the basis of the definition of the activity of the non-heat-treated sample (Control) as 100%. (C) Temperature dependence of azocaseinolytic activity. Activity assays were performed in buffer A for 10 min at the indicated temperatures using 0.5% azocasein as the substrate. (D) Temperature dependence of the activity toward suc-AAPK-pNA. The initial velocities (*vi*) of suc-AAPK-pNA (0.5 mM) hydrolysis catalyzed by the enzymes (0.1 μg/ml) were measured in buffer A over a temperature range of 30 to 90°C. The values are expressed as means ± SDs (bars) of the results of three independent experiments.

replacement of residue Arg276 with Ala results in destabilization of the enzyme. One possible explanation for the salt-induced precipitation and destabilization of pyrolysin is that the surface charge-charge interactions may be disturbed due to electrostatic screening; however, the precipitation and destabilization of pyrolysin occur at low concentrations of $CaCl_2$ (e.g., 10 mM) but at relatively high concentrations of NaCl (e.g., 600 mM), which correspond to an ionic strength of 0.03 M for 10 mM $CaCl_2$ and an ionic strength of 0.6 M for 600 mM NaCl, implying that the electrostatic screening effect is unlikely to play a major role in destabilizing pyrolysin. Instead, the effect of salts on pyrolysin stability appears to be attributed mainly to metal ion-protein interactions. Proteins are thought to contain many hard anionic head groups (e.g., —COO^- of Asp and Glu) and soft cationic head groups (e.g., —NH_3^+ of Lys and Arg), and the interaction of proteins with hard cations and soft anions, on average, is more pronounced than that with soft cations and hard anions (33). In this regard, the electrostatic attraction between a hard cation (e.g., Ca^{2+}, Mg^{2+}, or Na^+) and —COO^- is stronger than that between —NH_3^+ and —COO^-. Consequently, the presence of these metal ions may disturb the ion pairs formed between Asp/Glu and Lys/Arg, leading to the destabilization of pyrolysin. In addition, the effect of different ions on protein stability usually follows their ranking in the Hofmeister series, wherein Ca^{2+} and Mg^{2+} are more powerful hard cations than Na^+ (33). In agreement with this, our results also showed that Ca^{2+} and Mg^{2+} are stronger denaturants than Na^+ for pyrolysin. Notably, not all of the negatively charged residues on the surface of pyrolysin are involved in ion pair formation, and the inserts and C-terminal extension contain an even higher percentage (14 to 16%) of negatively charged residues, specifically, Asp residues, than the catalytic domain core (10%) (6). Thus, we cannot exclude the possibility that metal ions directly

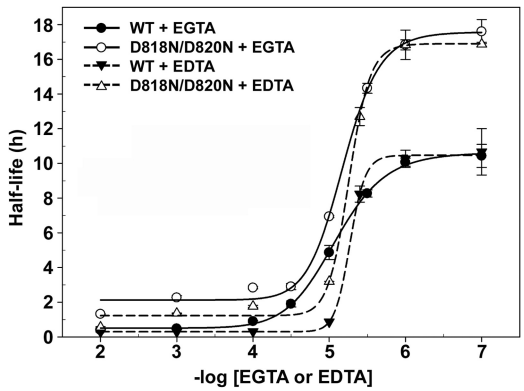

FIG 6 Chelator titration of the rate of inactivation of the WT and D818N/D820N mutant at 95°C. The enzymes (2.0 μg/ml) were incubated in buffer A containing different concentrations of EGTA or EDTA at 95°C. Residual activity toward azocasein was measured at appropriate time intervals, as described in Materials and Methods. Half-lives for thermal inactivation of the enzymes are plotted as a function of the negative log EGTA or EDTA concentration using the four-parameter logistic nonlinear regression model. The values are expressed as means ± SDs (bars) of the results of three independent experiments.

interact with these negatively charged residues to induce protein aggregation via attenuation of repulsive interactions between enzyme molecules.

Stabilization of pyrolysin by Ca^{2+} binding. Interestingly, Ca^{2+} also acts as a stabilizer of pyrolysin by binding to the enzyme at specific sites. Pyrolysin contains at least two Ca^{2+}-binding sites that play important roles in the Ca^{2+} binding and stability of pyrolysin. The fact that pyrolysin retains its hyperthermostability in the absence of supplemental Ca^{2+} but is destabilized by chelators suggests that the Ca^{2+}-binding sites of this enzyme have high affinities for Ca^{2+}. Similar results have been reported for hyperthermophilic Tk-SP subtilisin, to which the Ca^{2+} ions bind too tightly to be removed upon extensive dialysis against Ca^{2+}-free buffer but from which Ca^{2+} ions can be removed by treatment with EDTA (32).

The Ca1 site of pyrolysin corresponds to the Ca2 site of thermitase in terms of location within the enzyme, and two ligand residues (Asp55 and Asp58 in pyrolysin) are conserved between the two enzymes. In thermitase, however, the Ca2 site exhibits reduced Ca^{2+} binding in the absence of $CaCl_2$ and is considered a medium-strength Ca^{2+}-binding site (30). In the case of the pyrolysin Ca1 site, ligand residues originating from the inserts (e.g., Is147; Fig. 1A) that are located close to this site have been predicted to be involved in Ca^{2+} binding in combination with the conserved residues Asp55 and Asp58 (6). Moreover, our results demonstrate that the residue Glu59, which is located near Asp55 and Asp58 in pyrolysin but is absent in thermitase, also contributes to Ca^{2+} binding and plays a critical role in maintaining the thermal stability of pyrolysin. In this context, the Ca1 site of pyrolysin differs from the Ca2 site of thermitase in terms of the composition of ligand residues, which may account for the difference in their Ca^{2+}-binding affinities.

Four of the five ligand residues of the high-affinity Ca1 site of Tk-SP subtilisin are conserved in the pyrolysin Ca2 site (Asp818, Leu819, Asp820, and Glu842; Fig. 1A). The two Ca^{2+}-binding sites reside in the PPC domain of pyrolysin and in the β-jelly roll domain of Tk-SP subtilisin, and the two domains share ~25% sequence identity (23, 32). Both the PPC and β-jelly roll domain are located in the CTEs of the enzymes, and the CTEs have been confirmed to contribute to the structural stabilities of their cognate catalytic domains (23, 32). Here the disruption of the Ca2 site of pyrolysin, as in the case of the Ala substitution mutants (e.g., the D818A/D820A and D818A/D820A/E842A mutants), leads to the truncation of CTEm and the destabilization of the enzyme, indicating that binding of Ca^{2+} to the PPC domain is important for the global structure stability of pyrolysin. The molecular details of the stabilization of pyrolysin by its CTE, however, remain to be elucidated. Considering that pyrolysin is composed of a mosaic of domains, a plausible mechanism for this stabilization is that binding of Ca^{2+} increases the stability of the PPC domain and, in turn, stabilizes the global structure of the enzyme by modulating interdomain interactions.

Stability enhancement of pyrolysin with modification of the Ca2 site. Our results show that the removal of charged carboxyl groups at the Ca2 site leads to an increase in the thermostability of pyrolysin, such as in the cases of the D818N, D820N, D818N/D820N, and D818N/D820N/E842Q Asn substitution mutants. Most likely, the replacement of Asp with uncharged Asn reduced the electrostatic repulsion at the Ca2 site, leading to the increase in thermostability of the D818N/D820N mutant. According to the crystal structure of Tk-SP subtilisin, the Ca^{2+} ions are hexacoordinated with three side chain oxygen atoms of Asp460 ($O^{\delta1}$), Asp462 ($O^{\delta1}$), and Glu484 ($O^{\delta2}$); two main-chain carbonyl oxygen atoms from Leu461 and Thr478; and one water molecule in the Ca1 site (32). As mentioned above, the pyrolysin Ca2 site is highly similar to the Tk-SP subtilisin Ca1 site with respect to the composition of ligand residues. Given that the pyrolysin Ca2 site binds the Ca^{2+} ion in the same way, the replacement of Asp818 and Asp820 with uncharged Asn does not eliminate the Ca^{2+}-binding ligands, which may be provided by Asn ($O^{\delta1}$), but reduces the electrostatic repulsion at this site. This proposal is supported by the fact that the D818N/D820N mutant shows a similar apparent affinity for Ca^{2+} as the WT but is more stable than the latter. In contrast, upon elimination of the Ca^{2+}-binding ligands in the Ala substitution mutants (e.g., the D818A, D820A, and D818A/D820A mutants), the Ca^{2+}-binding affinity is reduced, leading to a decrease in enzyme stability. In the presence of chelators, unfavorable electrostatic repulsion between charged carboxyl groups at the Ca2 site of the WT would become more pronounced due to the depletion of Ca^{2+}, rendering the enzyme less stable than the Ala or Asn substitution mutants without charged carboxyl groups under chelating conditions. The improvement of protein stability by eliminating unfavorable electrostatic repulsion (Asp → Asn mutation) at Ca^{2+}-binding sites has also been described for other proteins, such as α-lactalbumin (34, 35).

Few studies have reported on the further stabilization of proteins from hyperthermophilic archaea. Vetriani and coworkers (36) successfully improved the thermostability of a glutamate dehydrogenase from *Thermococcus litoralis* by introducing an ion pair network that matches the structure of the more thermostable *P. furiosus* glutamate dehydrogenase. Similar results have been described for glutamate dehydrogenase from *T. kodakarensis* KOD1 (37). Recently, introduction of a single mutation (Glu99 → Gln) into the *Pyrococcus horikoshii* CutA1 protein was found to lead to an increase in the denaturation temperature of the protein, and the E99Q mutant was stabilized by deletion of the negatively charged group at the C terminus of an α helix, in addition to elimination of the repulsive interactions with the other two Glu residues (38). Here, the thermostability of pyrolysin was improved by elimination of unfavorable electrostatic repulsion in the Ca2 site. In all of these cases, the improvement of thermostability was achieved by optimization of the electrostatic interactions.

Stability versus activity. Pyrolysin is an extracellular enzyme produced by *P. furiosus* from geothermally heated marine sediments (16); however, recombinant pyrolysin tends to be destabilized and suffers autodegradation in the presence of metal ions at concentrations similar to those in seawater. This finding raises an interesting question of how pyrolysin functions in its natural environment. On the one hand, this question may be addressed from the perspective of the balance between the stability and activity of the enzyme. Enzyme stability and activity are generally correlated with its conformational flexibility, and an increase in flexibility, particularly around the active site, may cause enzyme destabilization but promotes enzyme activity by lowering the activation energy (39). In agreement with this notion, the metal ion-induced destabilization of recombinant pyrolysin is accompanied by an increase in enzyme activity. Most likely, destabilization of pyrolysin involves an increase in the local flexibility of the enzyme due to the disturbance of certain surface charge-charge interactions by metal ions. In this regard, metal ions play important roles in mod-

ulating the conformational flexibility of pyrolysin to improve its activity. On the other hand, the destabilizing effect of metal ions may be compensated for by other biotic or abiotic factors. Native pyrolysin is glycosylated and cell envelope associated, and most of the possible N-glycosylation sites are located outside the catalytic domain in either the large insert or the C-terminal extension (19, 21, 40). The evidence that the purified recombinant pyrolysin is less stable than native pyrolysin (23) suggests that the glycosylation and/or the association with the cell envelope play an important role in stabilizing the enzyme. Meanwhile, the glycosylation and the association with the cell envelope also render the enzyme less susceptible to autodegradation by limiting intermolecular proteolysis. In addition, the stabilization of the PPC domain by modification of the Ca2 site could increase both the global stability and the activity of the enzyme, even in ASW. This result led us to postulate that the stabilization of the global structure of native pyrolysin by external factors may be accompanied by further improvement of enzyme activity at high temperatures.

ACKNOWLEDGMENT

This work was supported by the National Natural Science Foundation of China (30470019).

REFERENCES

1. **Stetter KO, Fiala G, Huber G, Huber R, Segerer A.** 1990. Hyperthermophilic microorganisms. FEMS Microbiol. Lett. **75:**117–124. http://dx.doi.org/10.1111/j.1574-6968.1990.tb04089.x.
2. **Kashefi K, Lovley DR.** 2003. Extending the upper temperature limit for life. Science **301:**934. http://dx.doi.org/10.1126/science.1086823.
3. **Takai K, Nakamura K, Toki T, Tsunogai U, Miyazaki M, Miyazaki J, Hirayama H, Nakagawa S, Nunoura T, Horikoshi K.** 2008. Cell proliferation at 122°C and isotopically heavy CH_4 production by a hyperthermophilic methanogen under high-pressure cultivation. Proc. Natl. Acad. Sci. U. S. A. **105:**10949–10954. http://dx.doi.org/10.1073/pnas.0712334105.
4. **Atomi H, Sato T, Kanai T.** 2011. Application of hyperthermophiles and their enzymes. Curr. Opin. Biotechnol. **22:**618–626. http://dx.doi.org/10.1016/j.copbio.2011.06.010.
5. **Vieille C, Zeikus GJ.** 2001. Hyperthermophilic enzymes: sources, uses, and molecular mechanisms for thermostability. Microbiol. Mol. Biol. Rev. **65:**1–43. http://dx.doi.org/10.1128/MMBR.65.1.1-43.2001.
6. **Voorhorst WG, Warner A, de Vos WM, Siezen RJ.** 1997. Homology modelling of two subtilisin-like proteases from the hyperthermophilic archaea *Pyrococcus furiosus* and *Thermococcus stetteri*. Protein Eng. **10:**905–914. http://dx.doi.org/10.1093/protein/10.8.905.
7. **Daniel R, Dines M, Petach H.** 1996. The denaturation and degradation of stable enzymes at high temperatures. Biochem. J. **317:**1–11.
8. **Jaenicke R, Sterner R.** 2013. Life at high temperatures, p 337–374. *In* Rosenberg E, DeLong E, Lory S, Stackebrandt E, Thompson F (ed), The prokaryotes. Springer, Berlin, Germany.
9. **Yip KS, Stillman TJ, Britton KL, Artymiuk PJ, Baker PJ, Sedelnikova SE, Engel PC, Pasquo A, Chiaraluce R, Consalvi V, Scandurra R, Rice DW.** 1995. The structure of *Pyrococcus furiosus* glutamate dehydrogenase reveals a key role for ion-pair networks in maintaining enzyme stability at extreme temperatures. Structure **3:**1147–1158. http://dx.doi.org/10.1016/S0969-2126(01)00251-9.
10. **Ogasahara K, Lapshina EA, Sakai M, Izu Y, Tsunasawa S, Kato I, Yutani K.** 1998. Electrostatic stabilization in methionine aminopeptidase from hyperthermophile *Pyrococcus furiosus*. Biochemistry **37:**5939–5946. http://dx.doi.org/10.1021/bi973172q.
11. **Tahirov TH, Oki H, Tsukihara T, Ogasahara K, Yutani K, Ogata K, Izu Y, Tsunasawa S, Kato I.** 1998. Crystal structure of methionine aminopeptidase from hyperthermophile, *Pyrococcus furiosus*. J. Mol. Biol. **284:**101–124. http://dx.doi.org/10.1006/jmbi.1998.2146.
12. **Ren B, Tibbelin G, de Pascale D, Rossi M, Bartolucci S, Ladenstein R.** 1998. A protein disulfide oxidoreductase from the archaeon *Pyrococcus furiosus* contains two thioredoxin fold units. Nat. Struct. Mol. Biol. **5:**602–611. http://dx.doi.org/10.1038/862.
13. **Beeby M, O'Connor BD, Ryttersgaard C, Boutz DR, Perry LJ, Yeates TO.** 2005. The genomics of disulfide bonding and protein stabilization in thermophiles. PLoS Biol. **3:**e309. http://dx.doi.org/10.1371/journal.pbio.0030309.
14. **Unsworth LD, van der Oost J, Koutsopoulos S.** 2007. Hyperthermophilic enzymes—stability, activity and implementation strategies for high temperature applications. FEBS J. **274:**4044–4056. http://dx.doi.org/10.1111/j.1742-4658.2007.05954.x.
15. **Mayr J, Lupas A, Kellermann J, Eckerskorn C, Baumeister W, Peters J.** 1996. A hyperthermostable protease of the subtilisin family bound to the surface layer of the archaeon *Staphylothermus marinus*. Curr. Biol. **6:**739–749. http://dx.doi.org/10.1016/S0960-9822(09)00455-2.
16. **Fiala G, Stetter KO.** 1986. *Pyrococcus furiosus* sp. nov. represents a novel genus of marine heterotrophic archaebacteria growing optimally at 100°C. Arch. Microbiol. **145:**56–61. http://dx.doi.org/10.1007/BF00413027.
17. **Blumentals II, Robinson AS, Kelly RM.** 1990. Characterization of sodium dodecyl sulfate-resistant proteolytic activity in the hyperthermophilic archaebacterium *Pyrococcus furiosus*. Appl. Environ. Microbiol. **56:**1992–1998.
18. **Connaris H, Cowan DA, Sharp RJ.** 1991. Heterogeneity of proteinases from the hyperthermophilic archaeobacterium *Pyrococcus furiosus*. J. Gen. Microbiol. **137:**1193–1199. http://dx.doi.org/10.1099/00221287-137-5-1193.
19. **Eggen R, Geerling A, Watts J, de Vos WM.** 1990. Characterization of pyrolysin, a hyperthermoactive serine protease from the archaebacterium *Pyrococcus furiosus*. FEMS Microbiol. Lett. **71:**17–20. http://dx.doi.org/10.1111/j.1574-6968.1990.tb03791.x.
20. **Snowden LJ, Blumentals II, Kelly RM.** 1992. Regulation of proteolytic activity in the hyperthermophile *Pyrococcus furiosus*. Appl. Environ. Microbiol. **58:**1134–1141.
21. **Voorhorst WG, Eggen RI, Geerling AC, Platteeuw C, Siezen RJ, de Vos WM.** 1996. Isolation and characterization of the hyperthermostable serine protease, pyrolysin, and its gene from the hyperthermophilic archaeon *Pyrococcus furiosus*. J. Biol. Chem. **271:**20426–20431. http://dx.doi.org/10.1074/jbc.271.34.20426.
22. **Siezen RJ, Leunissen JA.** 1997. Subtilases: the superfamily of subtilisin-like serine proteases. Protein Sci. **6:**501–523.
23. **Dai Z, Fu H, Zhang Y, Zeng J, Tang B, Tang X-F.** 2012. Insights into the maturation of hyperthermophilic pyrolysin and the roles of its N-terminal propeptide and long C-terminal extension. Appl. Environ. Microbiol. **78:**4233–4241. http://dx.doi.org/10.1128/AEM.00548-12.
24. **Papworth C, Bauer J, Braman J, Wright D.** 1996. Site-directed mutagenesis in one day with >80% efficiency. Strategies **9:**3–4.
25. **Bradford MM.** 1976. A rapid and sensitive method for the quantitation of microgram quantities of protein utilizing the principle of protein-dye binding. Anal. Biochem. **72:**248–254. http://dx.doi.org/10.1016/0003-2697(76)90527-3.
26. **Laemmli UK.** 1970. Cleavage of structural proteins during the assembly of the head of bacteriophage T4. Nature **227:**680–685. http://dx.doi.org/10.1038/227680a0.
27. **Cheng G, Zhao P, Tang X-F, Tang B.** 2009. Identification and characterization of a novel spore-associated subtilase from *Thermoactinomyces* sp. CDF. Microbiology **155:**3661–3672. http://dx.doi.org/10.1099/mic.0.031336-0.
28. **Coelho SM, Scornet D, Rousvoal S, Peters NT, Dartevelle L, Peters AF, Cock JM.** 2012. How to cultivate *Ectocarpus*. Cold Spring Harb. Protoc. **2012:**258–261. http://dx.doi.org/10.1101/pdb.prot067934.
29. **DelMar EG, Largman C, Brodrick JW, Geokas MC.** 1979. A sensitive new substrate for chymotrypsin. Anal. Biochem. **99:**316–320. http://dx.doi.org/10.1016/S0003-2697(79)80013-5.
30. **Gros P, Kalk KH, Hol WG.** 1991. Calcium binding to thermitase. Crystallographic studies of thermitase at 0, 5, and 100 mM calcium. J. Biol. Chem. **266:**2953–2961.
31. **Teplyakov AV, Kuranova IP, Harutyunyan EH, Vainshtein BK, Wilson KS.** 1990. Crystal structure of thermitase at 1.4 Å resolution. J. Mol. Biol. **214:**261–279. http://dx.doi.org/10.1016/0022-2836(90)90160-N.
32. **Foophow T, Tanaka S, Angkawidjaja C, Koga Y, Takano K, Kanaya S.** 2010. Crystal structure of a subtilisin homologue, Tk-SP, from *Thermococcus kodakaraensis*: requirement of a C-terminal β-jelly roll domain for hyperstability. J. Mol. Biol. **400:**865–877. http://dx.doi.org/10.1016/j.jmb.2010.05.064.
33. **Kunz W.** 2010. Specific ion effects in colloidal and biological systems.

Curr. Opin. Colloid Interface Sci. **15:**34–39. http://dx.doi.org/10.1016/j.cocis.2009.11.008.
34. **Permyakov SE, Makhatadze GI, Owenius R, Uversky VN, Brooks CL, Permyakov EA, Berliner LJ.** 2005. How to improve nature: study of the electrostatic properties of the surface of α-lactalbumin. Protein Eng. Des. Sel. **18:**425–433. http://dx.doi.org/10.1093/protein/gzi051.
35. **Permyakov SE, Uversky VN, Veprintsev DB, Cherskaya AM, Brooks CL, Permyakov EA, Berliner LJ.** 2001. Mutating aspartate in the calcium-binding site of α-lactalbumin: effects on the protein stability and cation binding. Protein Eng. Des. Sel. **14:**785–789. http://dx.doi.org/10.1093/protein/14.10.785.
36. **Vetriani C, Maeder DL, Tolliday N, Yip KS-P, Stillman TJ, Britton KL, Rice DW, Klump HH, Robb FT.** 1998. Protein thermostability above 100°C: a key role for ionic interactions. Proc. Natl. Acad. Sci. U. S. A. **95:**12300–12305. http://dx.doi.org/10.1073/pnas.95.21.12300.
37. **Rahman RN, Fujiwara S, Nakamura H, Takagi M, Imanaka T.** 1998. Ion pairs involved in maintaining a thermostable structure of glutamate dehydrogenase from a hyperthermophilic archaeon. Biochem. Biophys. Res. Commun. **248:**920–926. http://dx.doi.org/10.1006/bbrc.1998.8933.
38. **Matsuura Y, Takehira M, Sawano M, Ogasahara K, Tanaka T, Yamamoto H, Kunishima N, Katoh E, Yutani K.** 2012. Role of charged residues in stabilization of *Pyrococcus horikoshii* CutA1, which has a denaturation temperature of nearly 150 °C. FEBS J. **279:**78–90. http://dx.doi.org/10.1111/j.1742-4658.2011.08400.x.
39. **D'Amico S, Marx JC, Gerday C, Feller G.** 2003. Activity-stability relationships in extremophilic enzymes. J. Biol. Chem. **278:**7891–7896. http://dx.doi.org/10.1074/jbc.M212508200.
40. **de Vos WM, Voorhorst WG, Dijkgraaf M, Kluskens LD, Van der Oost J, Siezen RJ.** 2001. Purification, characterization, and molecular modeling of pyrolysin and other extracellular thermostable serine proteases from hyperthermophilic microorganisms. Methods Enzymol. **330:**383–393. http://dx.doi.org/10.1016/S0076-6879(01)30390-7.